

# Deterministic High Order Vortex Methods for the 2D Navier–Stokes Equation with Rezoning

Henrik O. Nordmark

*Mathematics Department, Center of Research and Advanced Studies (CINVESTAV), Mexico City, Mexico*

Received February 22, 1995; revised January 22, 1996

---

In this paper, we extend the use of automatic rezoning to *viscous* flow in two dimensions. In a previous paper, we tested this technique on inviscid flow, with very good results. To simulate viscosity, we follow Fishelov’s idea of explicitly taking the Laplacian of the cutoff function, but unlike Fishelov we use a moving grid. This eliminates the need to approximate the gradient of the vorticity, but rezoning needs to be used to keep the discretization error low. We first test the method on a radially symmetric problem where the exact vorticity is known for all time. Using both an eighth order cutoff function and an infinite order cutoff function, we obtain low errors and high rates of convergence. Then, we calculate the evolution of two circular vortex patches and of a square vorticity patch. The exact solution for the last two problems is not known. In all test problems we use a viscosity coefficient of 0.0005. © 1996 Academic Press, Inc.

---

## 1. INTRODUCTION

Vortex methods are numerical methods for the Euler equations or the Navier–Stokes equations, which model incompressible fluid flow. The first such method, known as the *point vortex method*, was introduced by Rosenhead [15] in 1932 to calculate the behavior of vortex sheets. However, Rosenhead’s results were not accurate, because the method involved the spatial discretization of a *singular* integrodifferential equation. In 1973, Chorin [2] overcame the problem of the singularity by replacing the exact vorticity with the convolution of the vorticity with a “cutoff function,” which approximates the delta function. The advantage of this approach is that we are led to a smoother integrodifferential equation, which is then discretized with a smaller error. The price we pay for this is an additional error due to using the smoothed vorticity rather than the exact one. Nevertheless, this error is smaller than the discretization error, except possibly for a short initial time interval. Chorin [2] also introduced the technique of “random walk” to simulate viscosity. Although, it was long believed that point vortex methods were of little value, it has recently been proved that these methods do in fact converge. Hou, Lowengrub, and Shelley [8] presented an improved point vortex method, which gives quite good results for moderately long time integration.

Goodman [6] and Long [9] established the convergence of Chorin’s random vortex method. However, the rate of convergence for this method is low. Therefore, several types of *deterministic* vortex methods have been proposed in recent years by Fishelov [4], Cottet [3], and Cottet and Mas-Gallic [5], among others. Unlike most vortex methods, Fishelov’s method [4] uses a *fixed grid*. This approach requires the approximation of both the gradient and the Laplacian of the vorticity. This is achieved by explicitly taking the gradient and the Laplacian of the cutoff function. In this way, Fishelov [4] obtains much smaller numerical errors than for the random walk method.

The method in the present paper uses the same approximation as Fishelov [4] for the Laplacian of the vorticity, but it uses the more common movable grid rather than a fixed one. This simplifies the final equations. In particular, we do not need to calculate the vorticity gradient. The price for this is that the discretization error increases quite suddenly after a certain time interval. This occurs both for viscous and inviscid flow. In a previous article [11], the author overcame this problem, in the inviscid case, by using an automatic “rezoning” strategy. This means that we restart the time integration with a uniform grid when the vorticity error has grown by a certain percentage. In this paper, we extend this scheme to include the viscous case. To test the method, we need a test problem for which the exact vorticity or velocity is known as a function of time. The simplest case occurs when the initial vorticity is *radially symmetric*. The vorticity then satisfies the heat equation. Since the solution of the two-dimensional heat equation is in general only representable in terms of a double integral, previous authors [10, 14, and 4] have considered a point-wise comparison of the numerical vorticity with the exact one too “expensive.” Instead, they compared the second moment of the vorticity  $L(t) = \int_{R^2} |\mathbf{x}|^2 \omega(\mathbf{x}, t) d\mathbf{x} / \int_{R^2} \omega(\mathbf{x}, t) d\mathbf{x}$  with the corresponding discrete quantity, *based on the numerical vorticity*. This is motivated by the fact that  $L(t)$  has a very simple time dependence, given by  $L(t) = L(0) + 4\nu t$ . The main weakness of their approach is that while a large difference between the exact value of  $L(t)$  and the numerical value would indicate a large vortic-

ity error, a *small difference does not guarantee a small vorticity error*. This is because local vorticity errors may cancel each other out. Therefore, we feel that it is much more satisfactory to calculate the error at every point and then take the average in the  $L^2$  sense. As a matter of fact, the problem with discontinuous initial vorticity, studied by Roberts [14] and Fishelov [4], belongs to a class of problems for which the exact vorticity at any time  $t$  can be expressed in terms of convergent series, which can be readily evaluated. The first test problem in this paper belongs to the same class, but the initial vorticity is much smoother. When we tested our vortex method with rezoning on this problem, we found that high accuracy is maintained for large time integrations, just as in the inviscid case. In fact, the error grows a little slower in the viscous case, since the smoothness increases with time. We also considered two nonsymmetric problems for which the exact solutions are not known. Here, we estimated the accuracy by extrapolation. These estimates indicate that our method also works well on nonsymmetric problems.

## 2. THE NEW DETERMINISTIC METHOD

Consider the two-dimensional Navier–Stokes equation in vorticity–stream function form

$$\omega_t + \mathbf{u} \cdot \nabla \omega = \nu \Delta \omega, \quad (1)$$

$$\Delta \psi = -\omega, \quad (2)$$

$$u = \psi_y, \quad v = -\psi_x, \quad (3)$$

$$\operatorname{div}(\mathbf{u}) = 0, \quad (4)$$

where  $\mathbf{u} = (u, v)$  is the velocity vector,  $\mathbf{x} = (x, y)$  is the position vector,  $\omega$  is the vorticity,  $\psi$  is the stream function, and  $\nu$  is the kinematic viscosity. By solving the Poisson equation (2) and differentiating, we obtain the velocity as

$$\mathbf{u}(\mathbf{x}, t) = \int_{-\infty}^{\infty} \int_{-\infty}^{\infty} K(\mathbf{x} - \mathbf{z}) \omega(\mathbf{z}, t) d\mathbf{z}, \quad (5)$$

where

$$K(\mathbf{x}) = \frac{1}{2\pi r^2} \begin{pmatrix} -y \\ x \end{pmatrix}, \quad r = |\mathbf{x}|. \quad (6)$$

If the integral (5) is approximated by the trapezoidal rule, we are led to a system of ODEs which may, in principle, be solved by any standard ODE solver. This method is known as the *point vortex method*. However, since the kernel in (5) is singular, the discretization error will be quite large. To overcome this difficulty, Chorin [2] replaced the exact vorticity by the convolution of the vorticity with a so-called cutoff function  $\phi_\delta$ , depending on the parameter

$\delta$ , and which tends to the delta function in the sense of distributions as  $\delta$  tends to zero,

$$\tilde{\omega}(\mathbf{x}, t) = \omega * \phi_\delta = \int_{-\infty}^{\infty} \int_{-\infty}^{\infty} \phi_\delta(|\mathbf{x} - \mathbf{z}|) \omega(\mathbf{z}, t) d\mathbf{z}, \quad (7)$$

where  $\phi_\delta(r) = \phi(r/\delta)/\delta^2$ .

Substituting  $\tilde{\omega}$  instead of  $\omega$  in (5), we get an approximate velocity  $\tilde{\mathbf{u}}$ , which is the *exact velocity induced by  $\tilde{\omega}$* ,

$$\begin{aligned} \tilde{\mathbf{u}} &= K * \tilde{\omega} = K * \phi_\delta * \omega = K_\delta * \omega, \\ &= \int_{-\infty}^{\infty} \int_{-\infty}^{\infty} K_\delta(\mathbf{x} - \mathbf{z}) \omega(\mathbf{z}, t) d\mathbf{z}, \end{aligned} \quad (8)$$

where

$$K_\delta(\mathbf{x}) = K * \phi_\delta = f(r/\delta)K(\mathbf{x}), \quad (9)$$

$$f(r) = 2\pi \int_0^r \phi(s) ds. \quad (10)$$

If we now switch to Lagrangian variables, (8) becomes

$$\begin{aligned} \tilde{\mathbf{u}}(\mathbf{x}(\alpha, t), t) &= \int_{-\infty}^{\infty} \int_{-\infty}^{\infty} K_\delta(\mathbf{x}(\alpha, t) \\ &\quad - \mathbf{x}(\beta, t)) \omega(\mathbf{x}(\beta, t), t) d\beta, \end{aligned} \quad (11)$$

where  $\mathbf{x}(\beta, 0) = \beta \nabla \beta$ . The determinant of the Jacobian for this change of variables is 1, since the flow is incompressible. Discretizing (11) by the trapezoidal rule, with grid size  $h$ , we get

$$\tilde{\mathbf{u}}_i = \tilde{\mathbf{u}}(\mathbf{x}_i(t), t) \approx \sum_{\mathbf{j} \in \mathbf{Z} \times \mathbf{Z}} K_\delta(\mathbf{x}_i(t) - \mathbf{x}_j(t)) c_j(t), \quad (12)$$

where  $c_j(t) = \omega(\mathbf{x}_j(t), t)h^2$  and  $\mathbf{x}_j(0) = h\mathbf{j}$ . Since  $\tilde{\mathbf{u}}_i = d\tilde{\mathbf{x}}_i/dt$ , we get the following system of ODEs:

$$\frac{d\tilde{\mathbf{x}}_i}{dt} = \sum_{\mathbf{j} \in \mathbf{Z} \times \mathbf{Z}} K_\delta(\tilde{\mathbf{x}}_i(t) - \tilde{\mathbf{x}}_j(t)) \tilde{c}_j(t), \quad \text{where } \mathbf{i} \in \mathbf{Z} \times \mathbf{Z}. \quad (13)$$

To solve (13), we need a way to update the vorticity coefficients  $\tilde{c}_i(t)$ . We note that the left-hand side of (1) represents the time derivative of the vorticity along particle paths. In particular, the vorticity is constant along particle paths when the viscosity is zero. Since the vorticity is approximated by

$$\omega(\mathbf{x}, t) \approx \sum_{\mathbf{j} \in \mathbf{Z} \times \mathbf{Z}} \phi_\delta(\mathbf{x} - \mathbf{x}_j(t)) c_j(t), \quad (14)$$

we approximate its Laplacian by

$$\Delta \omega(\mathbf{x}, t) \approx \sum_{\mathbf{j} \in \mathbf{Z} \times \mathbf{Z}} \Delta \phi_\delta(\mathbf{x} - \mathbf{x}_j(t)) c_j(t). \quad (15)$$

We then get the following system of ODEs for the vorticity coefficients; see [4]:

$$\frac{d\tilde{c}_i}{dt} = \nu \sum_{\mathbf{j} \in \mathbf{Z} \times \mathbf{Z}} \Delta \phi_\delta(\tilde{\mathbf{x}}_i(t) - \tilde{\mathbf{x}}_j(t)) \tilde{c}_j(t) h^2, \quad \text{where } \mathbf{i} \in \mathbf{Z} \times \mathbf{Z}. \quad (16)$$

If we would like to follow the trajectories for some other particles  $\mathbf{z}_i$ , we also have to solve the system

$$\frac{d\tilde{\mathbf{z}}_i}{dt} = \sum_{\mathbf{j} \in \mathbf{Z} \times \mathbf{Z}} K_\delta(\tilde{\mathbf{z}}_i(t) - \tilde{\mathbf{x}}_j(t)) \tilde{c}_j(t), \quad \text{where } \mathbf{i} \in \mathbf{Z} \times \mathbf{Z}. \quad (17)$$

The basic method then consists of solving simultaneously the systems (13), (16), and, if desired, (17) with an appropriate ODE solver. In our experience, the classical fourth-order Runge–Kutta method works very well. Unfortunately, the basic method suffers from a substantial increase in the discretization error after a short time. In a previous article, the author proposed two automatic rezoning schemes to overcome this difficulty; see [11]. With a small modification, the same rezoning methods can be applied in this case. To monitor the vorticity error, we define

$$c_i^h(t) = h^2 \sum_{\mathbf{j} \in \mathbf{Z} \times \mathbf{Z}} \phi_\delta(\tilde{\mathbf{x}}_i(t) - \tilde{\mathbf{x}}_j(t)) \tilde{c}_j(t), \quad (18)$$

where  $\tilde{c}_j(t)$  is calculated by solving (16) and

$$E_\omega(t) = \left( h^2 \sum_{\mathbf{j} \in \mathbf{Z} \times \mathbf{Z}} (c_j^h(t) - \tilde{c}_j(t))^2 \right)^{1/2}. \quad (19)$$

Then  $c_i^h(t)$  approximates  $\omega(\tilde{\mathbf{x}}_i(t), t)h^2$  and  $E_\omega(t)$  is the discrete  $L^2$  norm of the vorticity coefficient error relative to the vorticity coefficients obtained from the numerical solution of (16). Let  $\eta$  be a parameter greater than unity. When  $E_\omega(t)/E_\omega(0) > \eta$ , we start over with a new uniform grid. The main issue here is how to determine the vorticity coefficients for the new grid. Suppose that  $t = T_1$  is the smallest value of  $t$  for which  $E_\omega(t)/E_\omega(0) > \eta$ . In version 1 we let

$$\tilde{c}_i(T_1)_{\text{new}} = h^2 \sum_{\mathbf{j} \in \mathbf{Z} \times \mathbf{Z}} \phi_\delta(h\mathbf{i} - \tilde{\mathbf{x}}_j(T_1)) \tilde{c}_j(T_1)_{\text{old}}. \quad (20)$$

We then “throw away” the old vortices and introduce new ones at the grid points  $\mathbf{x}_j(T_1) = h\mathbf{j}$ , deleting the ones for which the vorticity coefficient, according to (20), is smaller in absolute value than some parameter  $\varepsilon > 0$ . We then

again solve (13), (16), and (17), using the new vorticity coefficients. We continue this until  $E_\omega(t)/E_\omega(T_1) > \eta$ . Then we apply rezoning again. Version 2 differs from version 1 in the way the new vorticity coefficients are calculated. In version 2, we let

$$\tilde{c}_q(T_1)_{\text{new}} = h^2/4 \sum_{\mathbf{r} \in \frac{\mathbf{Z}}{2} \times \frac{\mathbf{Z}}{2}} \phi_\delta(h\mathbf{q} - \tilde{\mathbf{x}}_r(T_1)) \tilde{c}_r(T_1)_{\text{old}}. \quad (21)$$

This requires us to also track vortices with index  $\mathbf{q} \in \mathbf{Z}/2 \times \mathbf{Z}/2$ . Therefore, we solve (13), (16), and (17)  $\forall \mathbf{i} \in \mathbf{Z}/2 \times \mathbf{Z}/2$  rather than just  $\mathbf{i} \in \mathbf{Z} \times \mathbf{Z}$ , as long as the vorticity coefficients have absolute value greater than  $\varepsilon$ . Note, however, that we still assume that  $\mathbf{j} \in \mathbf{Z} \times \mathbf{Z}$ ; i.e., the sums in (13), (16), and (17) are taken only over indices in  $\mathbf{Z} \times \mathbf{Z}$ . For more details see [11, pp. 372–376]. In the numerical calculations for this paper, we have used “version 2” throughout.

### 3. NUMERICAL RESULTS

We present three test problems. In the first one, the flow is radially symmetric, and the exact vorticity and angular velocity of the flow are known for every  $t$ , in terms of various convergent series. Therefore, we can calculate the numerical error exactly in this case. The other two test problems are not radially symmetric, and the exact solutions for these are unknown. Here, we show the numerical solution graphically, and the rate of convergence is estimated by extrapolation. For time integration, we used the classical fourth-order Runge–Kutta method throughout. The viscosity coefficient  $\nu$  is taken to be 0.0005 in all test problems. The initial vorticity for the first test problem is given by

$$\begin{aligned} \omega(r, 0) &= (1 - r^2)^k & \text{for } r \leq 1, \\ &= 0 & \text{for } r > 1. \end{aligned} \quad (22)$$

This initial condition has been considered by several authors for *inviscid* flow, for example [1, 13, 11]. Here, we choose  $k = 7$ , but for the sake of generality we will give the exact solution for arbitrary integer  $k$ . Note that  $k = 0$  corresponds to the discontinuous initial condition considered in [14, 4]. As in the inviscid case, the velocity of a fluid particle is related to its position by

$$(u(x(t), y(t)), v(x(t), y(t)))^T = \mu(r, t)(-y(t), x(t))^T, \quad (23)$$

where

$$\mu(r, t) = \frac{1}{r^2} \int_0^r s \omega(s, t) ds \quad (24)$$

is the angular velocity. Now, the position vector  $(x(t), y(t))$  is given by

$$x(t) = x(0) \cos(\theta(r, t)) - y(0) \sin(\theta(r, t)), \quad (25)$$

$$y(t) = x(0) \sin(\theta(r, t)) + y(0) \cos(\theta(r, t)), \quad (26)$$

where

$$\theta(r, t) = \int_0^t \mu(r, s) ds \quad (27)$$

is the total angle. The exact vorticity can be expressed by either of the series,

$$\omega(r, t) = (4\nu t)^k e^{-(r^2+1)/4\nu t} \sum_{n=k+1}^{\infty} \frac{(n-1)! I_n(r/2\nu t)}{(n-1-k)! r^n}, \quad (28)$$

$$= \sum_{n=0}^k \frac{k!}{(k-n)!} (-4\nu t)^n L_n(-r^2/4\nu t) \quad (29)$$

$$- (-4\nu t)^k e^{-(r^2+1)/4\nu t} \sum_{n=0}^{\infty} \frac{(n+k)!}{n!} r^n I_n(r/2\nu t),$$

$$= -k! e^{-r^2/4\nu t} \sum_{n=0}^{\infty} \frac{L_n(r^2/4\nu t)}{(n+k+1)! (-4\nu t)^{n+1}}, \quad (30)$$

where  $I_n$  is the modified Bessel function of order  $n$  and  $L_n$  the Laguerre polynomial of degree  $n$ . Using the bound for modified Bessel functions

$$|I_n(x)| \leq \frac{\sqrt{\pi}|x/2|^n e^x}{(n-1)!}, \quad (31)$$

we easily find that (28) is majorized (up to a constant) by the Taylor series for  $e^{1/(4\nu t)}$  and thus converges  $\forall t > 0$ . A large number of terms may be required if  $\nu t$  is small, but if  $r > 1$  we can use the bound  $|I_n(x)| \leq e^x$  to show that the whole series (28) is bounded by  $(4\nu t)^k k! e^{-(r-1)^2/(4\nu t)} (r-1)^{-(k+1)}$ . Hence, the vorticity is negligible if  $r > 1 + \delta$  and  $\nu t$  is ‘‘small enough.’’ The same argument shows that for the same small value of  $\nu t$ , the second sum in (29) is negligible when  $r < 1 + \delta$ . Therefore, the only difficult case is when both  $\nu t$  is small and  $r$  is close to 1. Even in this case, the CPU time required to calculate the exact solution is very small compared to the overall CPU time used in implementing the vortex method. It is also possible to use an asymptotic expansion when  $\nu t$  is small and  $r$  is close to 1, given in [12]. In [12] we also find the Taylor series of  $\omega(r, t)$  with respect to  $r$  about  $r = 0$  and  $r = 1$ , but these are less useful because the coefficients are hypergeometric functions of  $t$ . The angular velocity is ob-

tained by integrating (28)–(30) term by term. We get

$$\mu(r, t) = \frac{1 - (4\nu t)^{k+1} e^{-(r^2+1)/4\nu t} \sum_{n=k+1}^{\infty} \frac{n! I_n(r/2\nu t) / ((n-1-k)! r^n)}{2(k+1)r^2}, \quad (32)$$

$$= \frac{1}{2} \sum_{n=0}^k \frac{k! (-4\nu t)^n L_n^{(1)}(-r^2/4\nu t)}{(k-n)! (n+1)} + \frac{(-4\nu t)^{k+1} e^{-(r^2+1)/4\nu t}}{2(k+1)r^2} + \sum_{n=0}^{\infty} \frac{(n+k+1)! r^{n+1} I_{n+1}(r/2\nu t)}{n!}, \quad (33)$$

$$= \frac{1 - e^{-r^2/4\nu t}}{2(k+1)r^2} - k! e^{-r^2/4\nu t} \sum_{n=1}^{\infty} \frac{L_{n-1}^{(1)}(r^2/4\nu t)}{2n(n+k+1)! (-4\nu t)^{n+1}}. \quad (34)$$

In the numerical solution, we use two different cutoff functions, namely Hald’s infinite order cutoff function

$$\phi(r) = \frac{4}{45\pi r^3} (16J_3(4r) - 10J_3(2r) + J_3(r)), \quad (35)$$

where  $J_3$  is the Bessel function of order 3, and Nordmark’s eighth-order cutoff function

$$\phi(r) = \begin{cases} 52(r^2 - 1)^9 (140r^6 - 105r^4 + 21r^2 - 1) / \pi & \text{for } 0 \leq r \leq 1, \\ 0 & \text{for } r \geq 1. \end{cases} \quad (36)$$

It is well known that the smoothing error increases as  $\delta$  increases, while the reverse is true for the discretization error. For high order cutoff functions these two errors are approximately balanced if  $\delta$  is taken proportional to  $\sqrt{h}$ , as long as the vorticity is smooth enough; see [7]. This is the case here. Indeed, since the vorticity satisfies the heat equation in the radially symmetric case, it is analytic in  $r$  for  $t > 0$ . Therefore, we will take  $\delta$  proportional to  $\sqrt{h}$  throughout this paper. Most authors use  $\delta = h^q$ , with  $q$  only slightly less than unity. This is appropriate if the order of the cutoff function is not so high, or if the vorticity is not very smooth. With our choice of  $\delta$ , we expect that the velocity error will be of order  $O(h^4)$  for the eighth-order cutoff function, and of order  $O(h^\infty)$ , i.e., the error tends to 0 faster than any power of  $h$ , for the infinite order cutoff function. When the rate of convergence is finite, it can be

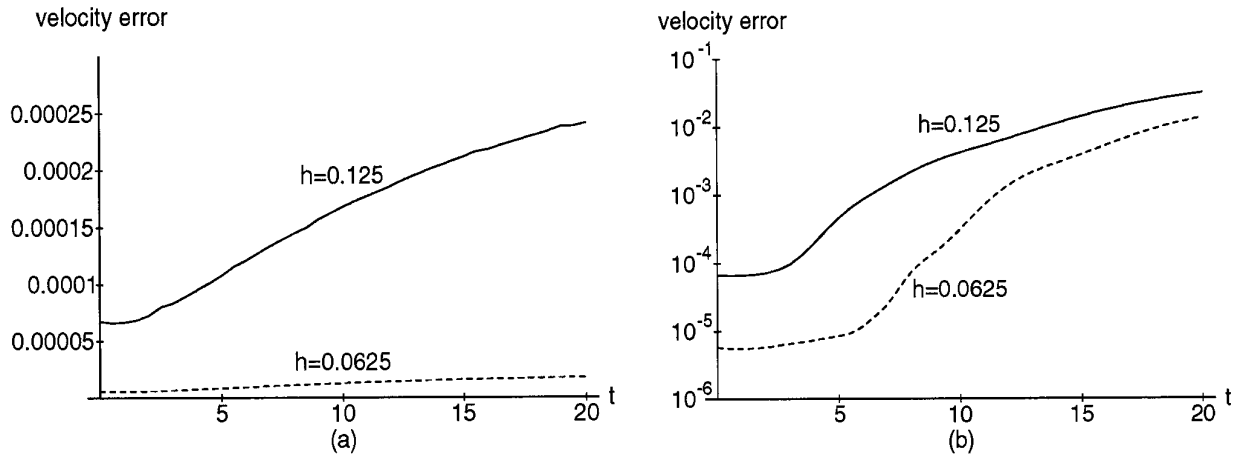


**FIG. 1.** Velocity errors in the discrete  $L^2$  norm as a function of time, with eighth-order cutoff function and  $\delta = 2.2\sqrt{h}$  with rezoning (a) and without rezoning (b). Note the logarithmic scale in (b).

estimated by

$$\text{rate of convergence} \approx \frac{\ln(\text{error}(h_1)/\text{error}(h_2))}{\ln(h_1/h_2)}. \quad (37)$$

For infinite (exponential) rate of convergence, (37) is not valid but for simplicity, we will still use (37) as the “observed” rate of convergence even in this case, with  $h_1 = \frac{1}{8}$  and  $h_2 = \frac{1}{16}$ . Although the solution is analytic for *any*  $t > 0$ , the numerical method will not “feel” this for small values of  $t$ . In more precise terms, the derivatives at  $r = 1$  of order higher than 7 will be very large for small  $t$ , but will gradually get smaller as  $t$  gets larger. Therefore, we expect the observed rate of convergence to increase with increasing time when using the infinite order cutoff function. Figures 1a–6a give the velocity and vorticity errors and observed rate of convergence for the first test problem,

with rezoning, using the eighth-order cutoff function and two different values of the parameter  $\delta$ . For comparison, we give the corresponding results *without* rezoning in Figs. 1b–6b. The errors in Figs. 1b, 2b, 4b, and 5b are plotted on a logarithmic scale. This is necessary, since the errors increase by several orders of magnitude when no rezoning is applied. We note that initially, both the velocity and the vorticity errors are smaller for the smaller value of  $\delta$ . This is because the smoothing error, which decreases with decreasing  $\delta$ , dominates over the discretization error in the beginning. However, if no rezoning is used, we eventually get higher errors with the smaller value of  $\delta$ , as the discretization error becomes larger than the smoothing error more quickly in this case. But although the errors without rezoning grow less rapidly with the larger value of  $\delta$ , they still become too large. Looking at Fig. 3b, we see that the observed rates of convergence get much larger

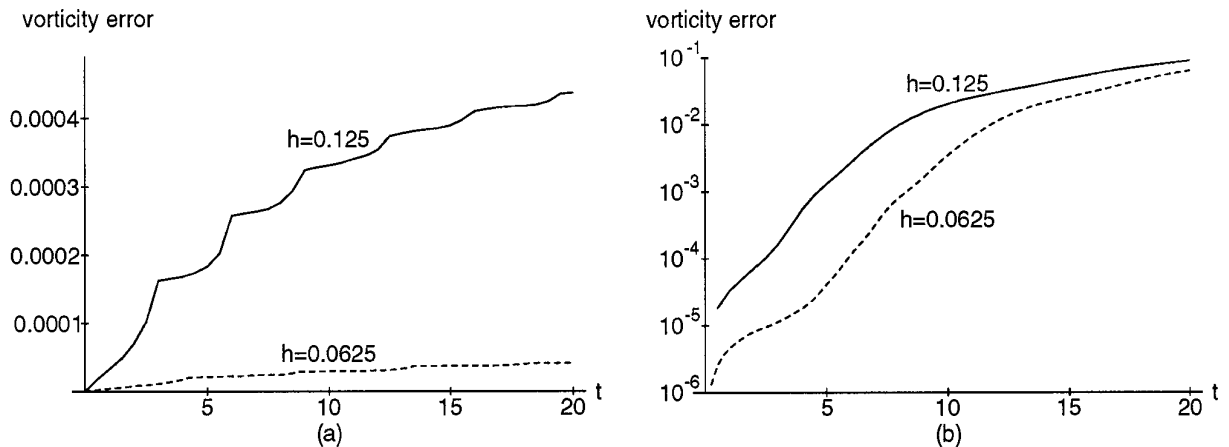
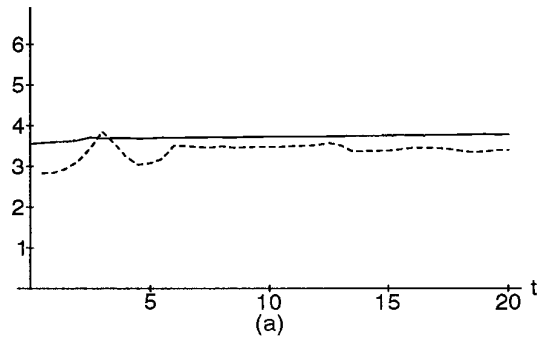


**FIG. 2.** Vorticity errors in the discrete  $L^2$  norm as a function of time, with eighth-order cutoff function and  $\delta = 2.2\sqrt{h}$  with rezoning (a) and without rezoning (b).

Rate of Convergence



Rate of Convergence

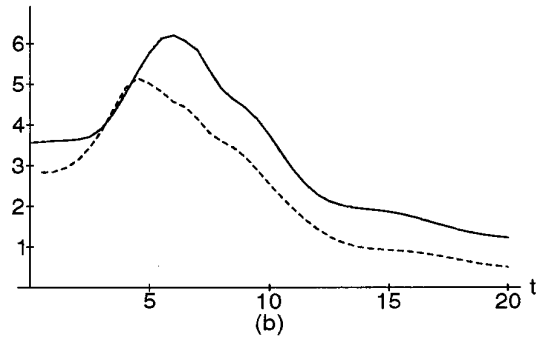
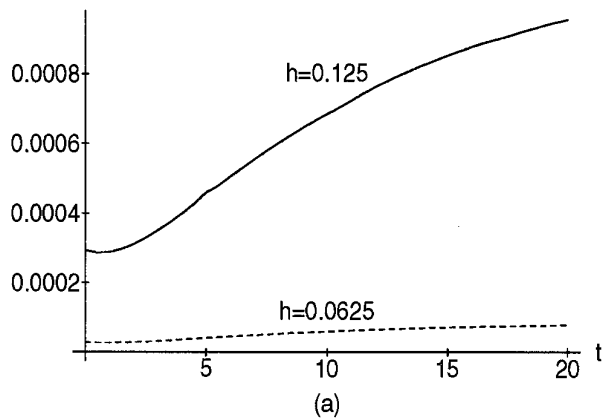


**FIG. 3.** Estimated rates of convergence for the velocity (solid curve) and the vorticity (dashed curve), with eighth-order cutoff function and  $\delta = 2.2\sqrt{h}$  with rezoning (a) and without rezoning (b).

velocity error



velocity error

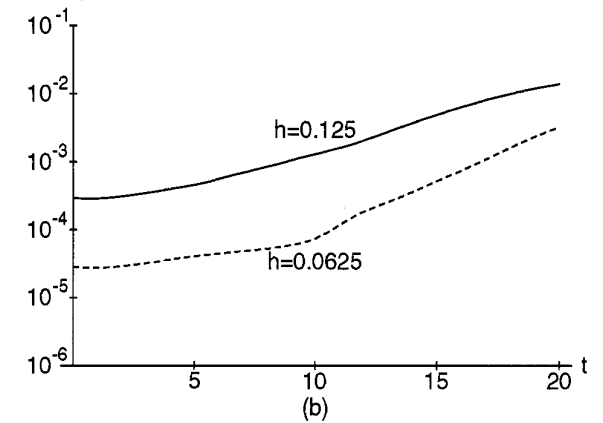
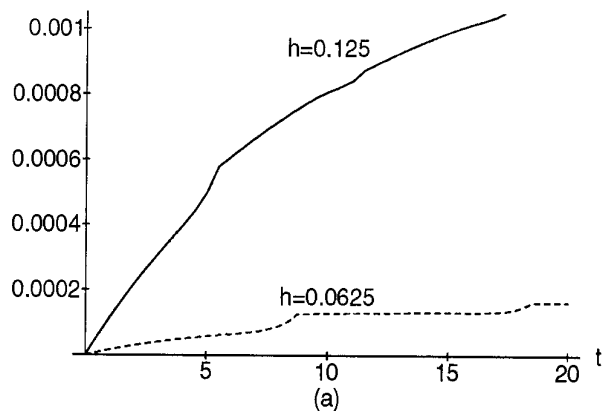


**FIG. 4.** Velocity errors with eighth-order cutoff function and  $\delta = 2.75\sqrt{h}$  with rezoning (a) and without rezoning (b).

vorticity error



vorticity error

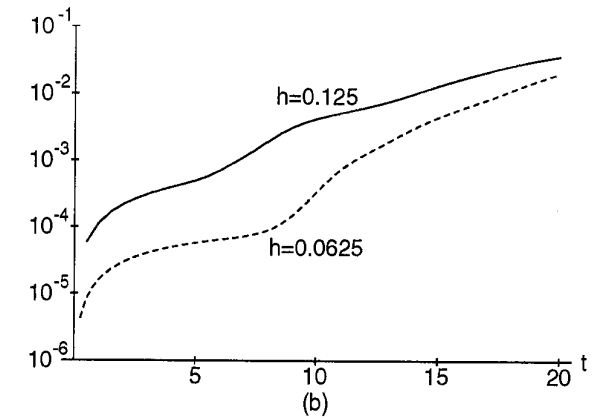


**FIG. 5.** Vorticity errors with eighth-order cutoff function and  $\delta = 2.75\sqrt{h}$  with rezoning (a) and without rezoning (b).

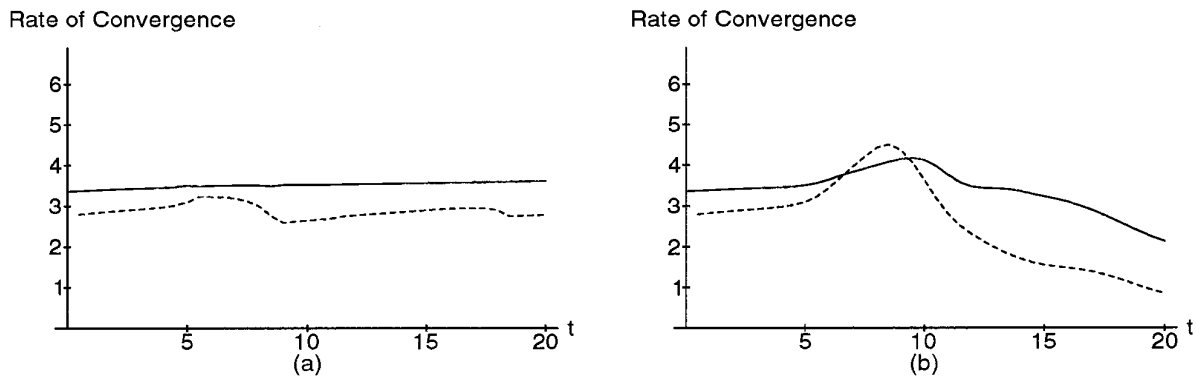


**FIG. 6.** Estimated rates of convergence for the velocity (solid curve) and the vorticity (dashed curve), with eighth-order cutoff function and  $\delta = 2.75\sqrt{h}$  with rezoning (a) and without rezoning (b).

around  $t = 5$ , before dropping off sharply. This is only because the errors increase sooner for  $h = 0.125$  than for  $h = 0.0625$ . However, eventually the errors grow relatively more for  $h = 0.0625$ , causing the drop in the observed rates of convergence. Let us see what happens when we *do* use rezoning. In Figs. 1a–6a we see that the errors for larger values of  $t$  are several orders of magnitude smaller than without rezoning. Furthermore, the smaller value of  $\delta$  now gives us smaller errors over the entire time interval, although a greater number of rezonings are necessary. This does not mean that  $\delta$  can be taken arbitrarily small, for if  $\delta$  is taken too small, the discretization error would dominate even at  $t = 0$ . The irregularities in Figs. 1a–6a occur precisely when rezoning takes place, because the errors either drop or increase more slowly after rezoning. These irregularities are absent when no rezoning is used, as we see in Figs. 1b–6b. Comparing Figs. 3a and 6a we note that, the observed rate of convergence of the velocity is now nearly constant in time, around 3.5, both for  $\delta = 2.2\sqrt{h}$  and  $\delta = 2.75\sqrt{h}$ . The observed rate of convergence of the

vorticity is more variable in time, but is in general somewhat lower than the velocity rate.

For the infinite order cutoff function, we still use  $\delta$  proportional to  $\sqrt{h}$ , but the proportionality factor must be much smaller. This is because  $\phi_\delta(0) = 7/(4\pi\delta^2)$  for the infinite order cutoff function, but for the eighth-order cutoff function  $\phi_\delta(0) = 52/(\pi\delta^2)$ , i.e.,  $208/7$  times larger, if the same value of  $\delta$  is used. To compensate for this, we take  $\delta$  smaller by a factor of  $\sqrt{208/7} \approx 5.5$  for the infinite order cutoff function, see [11, pp. 371–372]. Therefore, we use  $\delta = 0.4\sqrt{h}$  and  $\delta = 0.5\sqrt{h}$ , respectively. The errors and rates of convergence with rezoning are given in Figs. 7a–12a, and the corresponding results without rezoning in Figs. 7b–12b. We note that when rezoning is used, the maximum errors are smaller than for the eighth-order cutoff function, especially for  $h = 0.0625$ . The observed rates of convergence are also higher, and now increase with time, as the flow gets smoother. For the eighth-order cutoff function, this increase in the rates of convergence did not take place, since the rates were limited by the

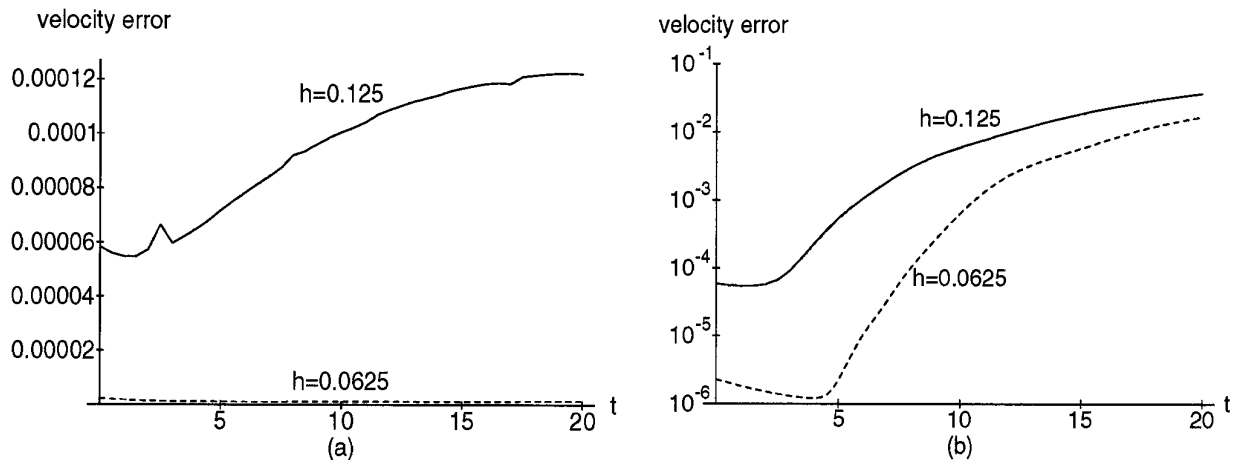


**FIG. 7.** Velocity errors with infinite order cutoff function and  $\delta = 0.4\sqrt{h}$  with rezoning (a) and without rezoning (b).

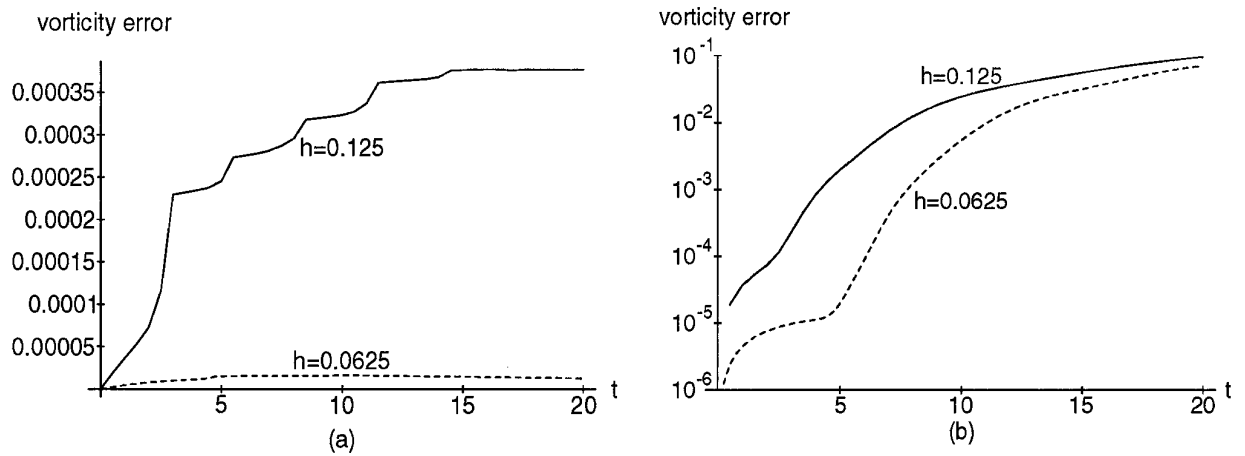


FIG. 8. Vorticity errors with infinite order cutoff function and  $\delta = 0.4\sqrt{h}$  with rezoning (a) and without rezoning (b).

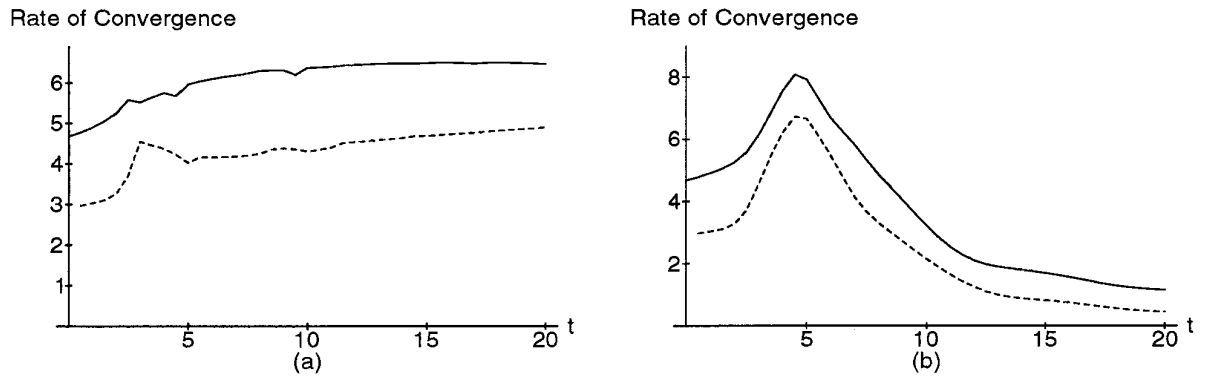


FIG. 9. Estimated rates of convergence for the velocity (solid curve) and the vorticity (dashed curve), with infinite order cutoff function and  $\delta = 0.4\sqrt{h}$  with rezoning (a) and without rezoning (b).

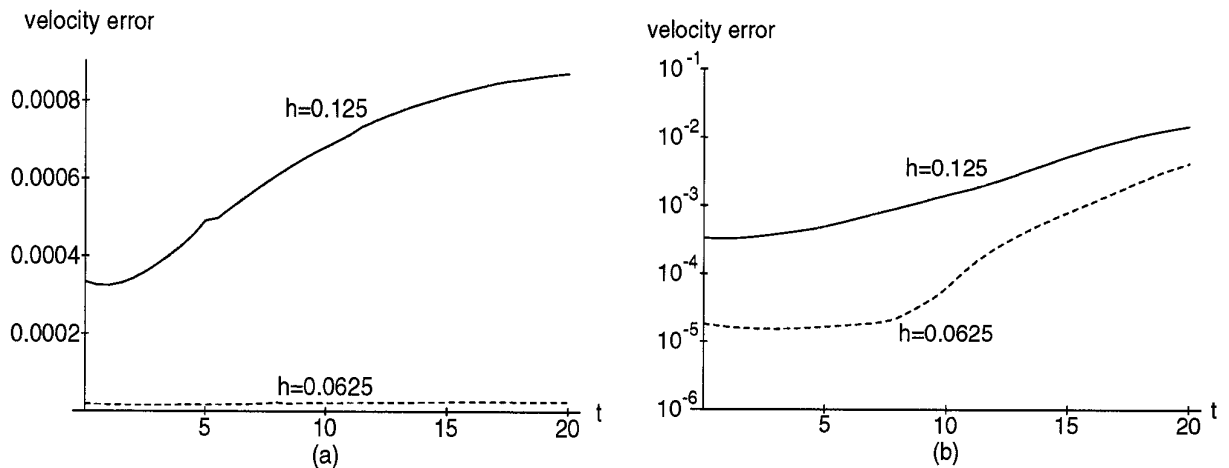


FIG. 10. Velocity errors with infinite order cutoff function and  $\delta = 0.5\sqrt{h}$  with rezoning (a) and without rezoning (b).



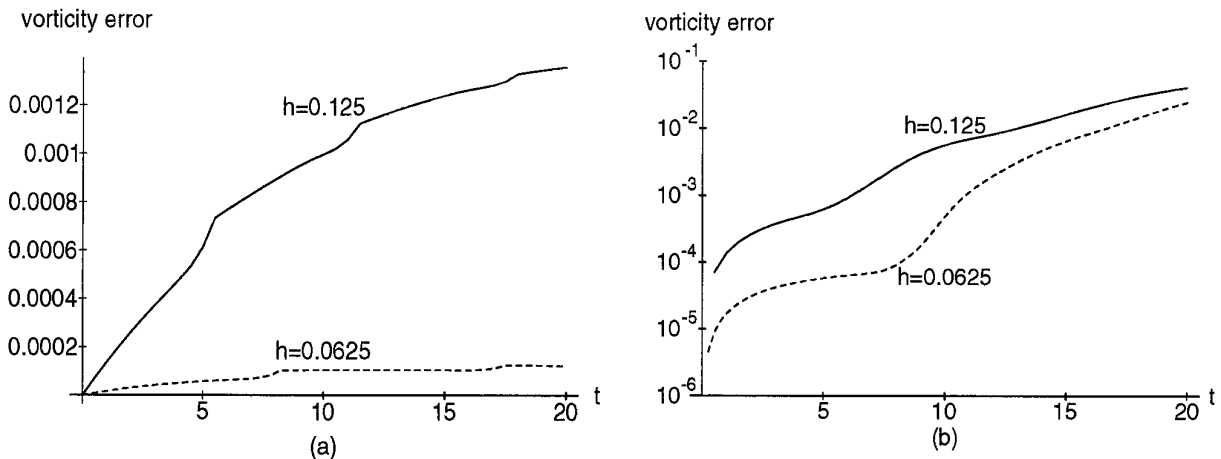


FIG. 11. Vorticity errors with infinite order cutoff function and  $\delta = 0.5\sqrt{h}$  with rezoning (a) and without rezoning (b).

cutoff function itself. On the other hand, if no rezoning is applied, the advantage of the infinite order cutoff function gets lost after a short time, and eventually the errors become as large as for the eighth-order cutoff function. The rates of convergence also drop off. This agrees with what has been observed by other authors, for example, Perlman [13] and Beale and Majda [1]. Hence, there is not much point in using a higher order cutoff function in the original vortex method.

Before moving on to the second test problem, let us see what happens if we use  $\delta = 2.2\sqrt{h}$  and  $\delta = 2.75\sqrt{h}$  for the infinite order cutoff function. As we see in Fig. 13, the results are poor. This is because the values of  $\delta$  are far too large for this cutoff function. As a consequence, the smoothing error becomes large, while the discretization error is negligible, even for later times. We also note that in this case there is in practice no distinction between the vortex method with automatic rezoning and the basic method. Indeed, even if automatic rezoning is in effect, it will never take place because the relative vorticity error  $E_\omega(t)$  remains nearly constant.

In the second test problem, we use two initially circular vortices with the initial condition given by

$$\omega(x, y, 0) = (\max(0, (1 - 4(|x| - 0.5)^2 - 4y^2)))^7. \quad (38)$$

The viscosity coefficient is again taken to be 0.0005, and we use the infinite order cutoff function. The parameter  $\delta$  is taken slightly smaller than in the first problem, namely  $\delta = 0.3\sqrt{h}$ . This is to compensate for the fact that in the current problem, each of the two vortices has an initial diameter 1, while the initial diameter of the vortex in the first problem is 2. Furthermore, this choice of  $\delta$  results in a reasonable “rezoning frequency.” Figure 14 shows the positions of marker particles at different times. These positions were obtained by solving the system of ODEs (17) for 3270 particles (denoted by  $\mathbf{z}_i$  in (17)), initially distributed on two sets of concentric circles. The positions of these 3270 particles are then connected by the graphics software at each time level except  $t = 0$ , to obtain the closed curves. Unlike the case of inviscid flow,

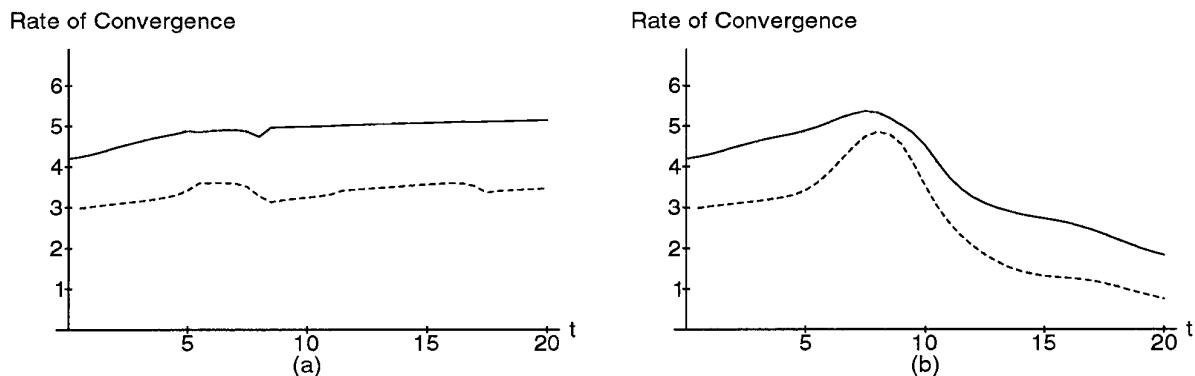


FIG. 12. Estimated rates of convergence for the velocity (solid curve) and the vorticity (dashed curve), with infinite order cutoff function and  $\delta = 0.5\sqrt{h}$  with rezoning (a) and without rezoning (b).

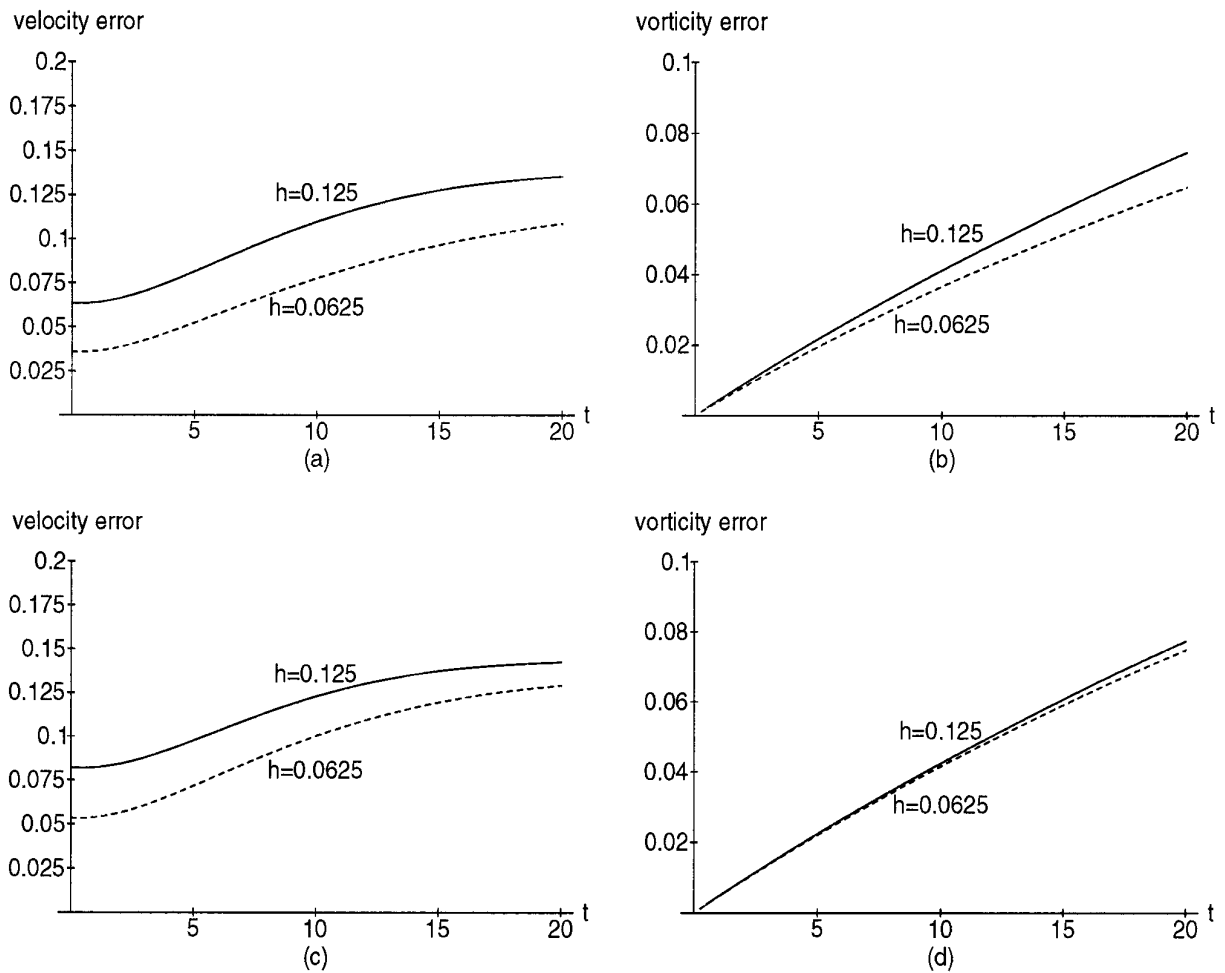


FIG. 13. Velocity and vorticity errors with the infinite order cutoff function and  $\delta = 2.2\sqrt{h}$ , (a), (b), and  $\delta = 2.75\sqrt{h}$ , (c), (d).

the vorticity *is not* constant along particle paths in viscous flow. Hence, the closed curves do not necessarily represent contours of constant vorticity, except at time  $t = 0$ . We note that the curves remain smooth even at large times. This is because of the large number of particles used and the fact that particles which are initially “close together,” remain close. In other words, there is not much “stretching.” This is probably a consequence of the high degree of smoothness of the flow and contrasts sharply with the inviscid version of the same problem, which was studied by the author in [11]. In the inviscid case, there was so much stretching at later times that it was no longer possible to obtain an accurate picture of the flow by connecting adjacent points.

In the current problem, we cannot calculate the numerical errors exactly, but we can estimate the errors and the rates of convergence by using extrapolation. To do this,

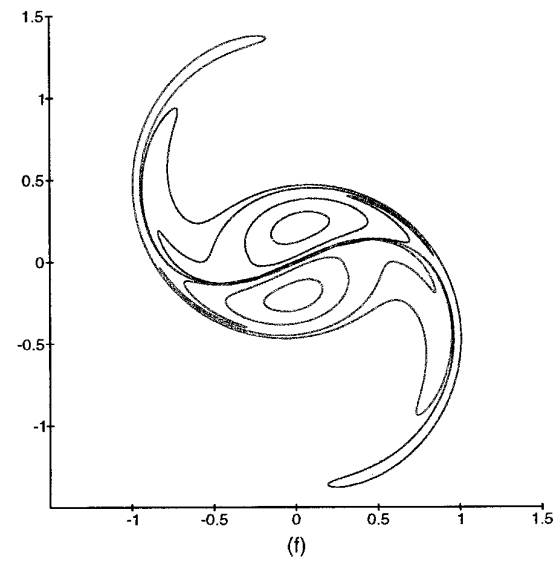
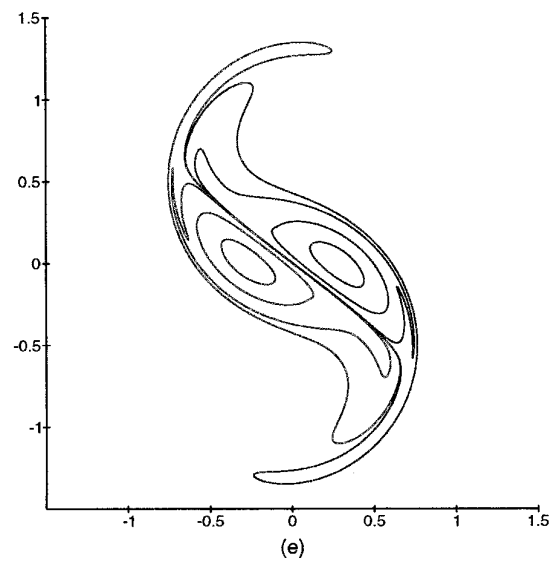
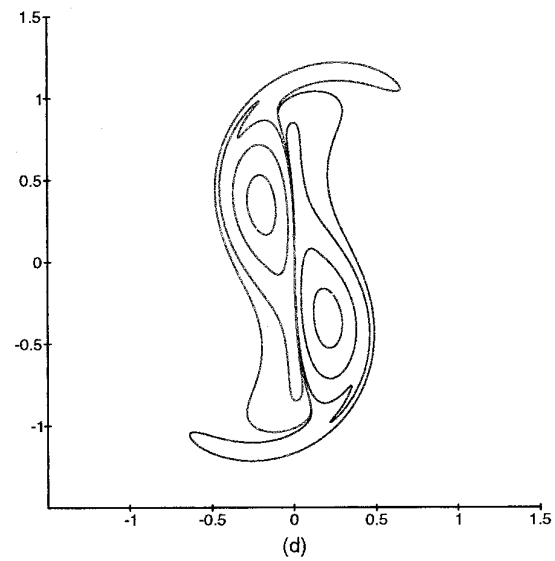
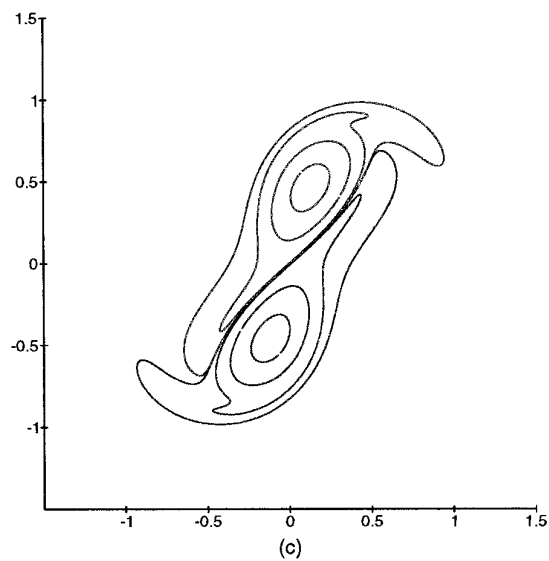
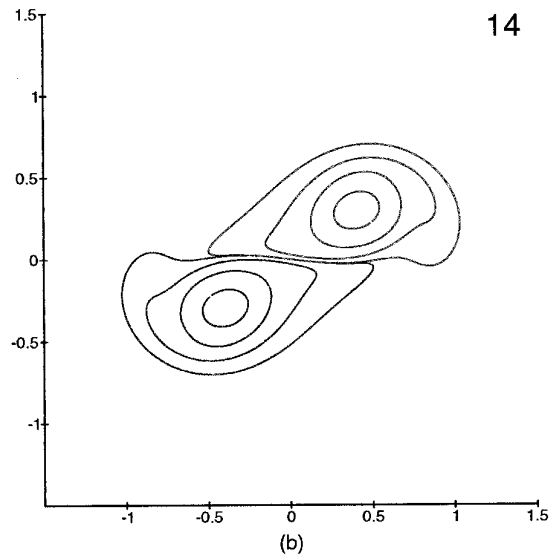
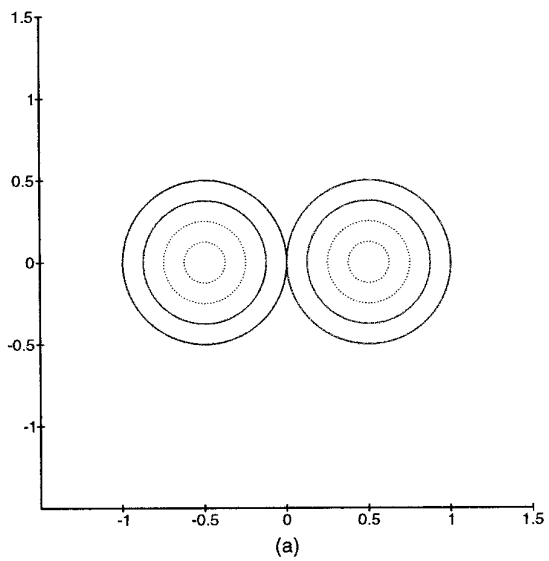
we use three grids with gridsizes  $h_1 = \frac{1}{8}$ ,  $h_2 = 3h_1/4 = \frac{1}{12}$  and  $h_3 = 9h_1/16 = \frac{1}{16}$ , respectively. We assume that the spatial rate of convergence is  $q$  and that the numerical velocity is given by  $\tilde{\mathbf{u}}_i = \mathbf{u}_i + h^q e_1(\mathbf{x}_i, t) + (\Delta t)^4 e_2(\mathbf{x}_i, t) +$  (higher order terms). Then

$$\frac{\|\tilde{\mathbf{u}}_i^{h_1} - \tilde{\mathbf{u}}_i^{h_2}\|}{\|\tilde{\mathbf{u}}_i^{h_2} - \tilde{\mathbf{u}}_i^{h_3}\|} \sim \frac{h_1^q - (3h_1/4)^q}{(3h_1/4)^q - (9h_1/16)^q} = \left(\frac{4}{3}\right)^q, \quad (39)$$

from which  $q$  is estimated by taking the logarithm of both sides. Once we have estimated  $q$  we can readily estimate  $e_1(\mathbf{x}_i, t)$ . Then, by assuming the error due to time discretization is much smaller than the spatial error, which is indeed the case for the values of  $\Delta t$  used, an approximate velocity error is given by  $h^q e_1(\mathbf{x}_i, t)$ . We proceed in the same fashion for the vorticity error and rate of convergence. Figure 15

FIG. 14. Particle positions at  $t = 0$  (a),  $t = 20$  (b),  $t = 40$  (c),  $t = 60$  (d),  $t = 80$  (e), and  $t = 100$  (f), with infinite order cutoff function.  $\omega(x, y, 0) = \max(0, (1 - 4(|x| - 0.5)^2 - 4y^2))^7$ ,  $h = 0.0625$ ,  $\delta = 0.3\sqrt{h}$ ,  $\Delta t = 4.0h$ .

14



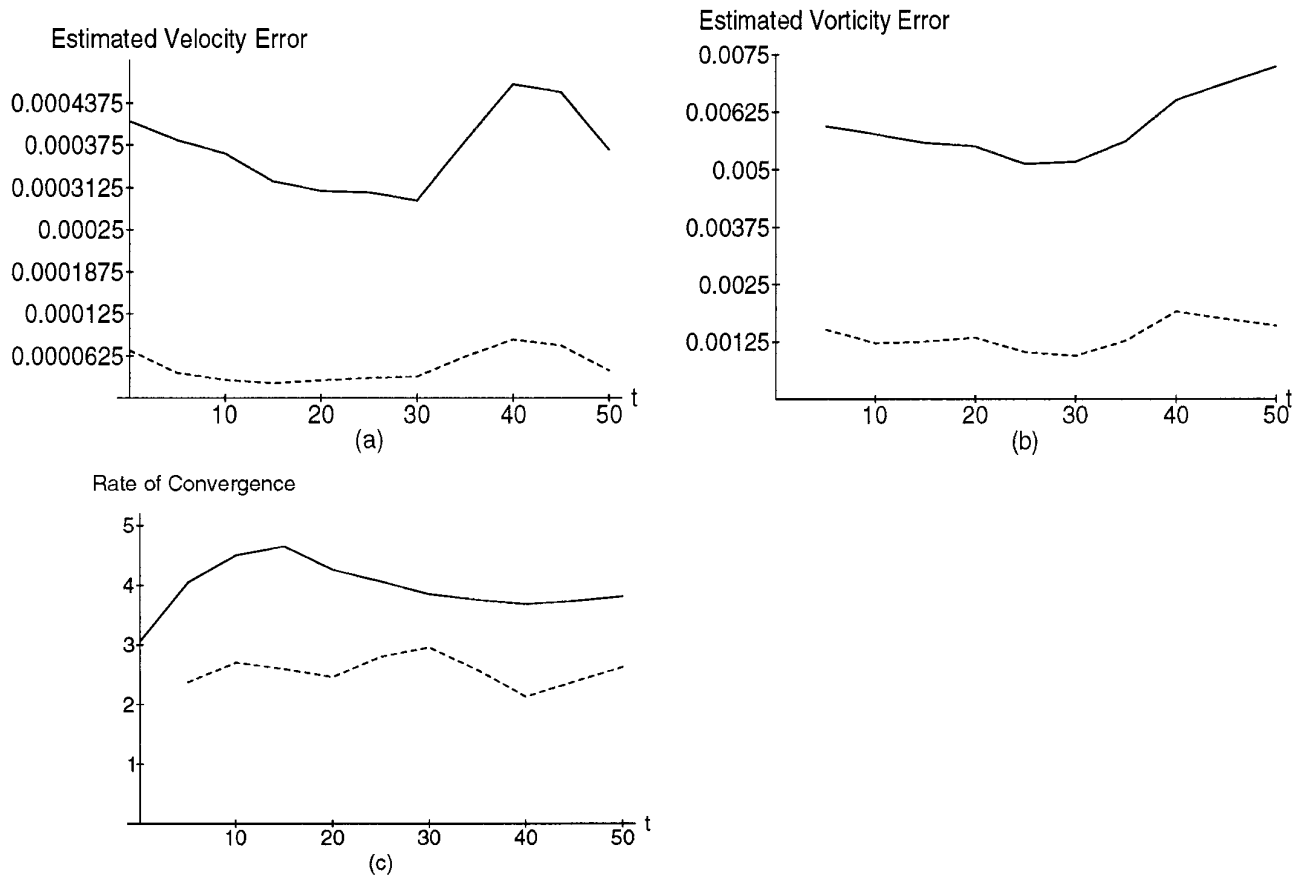


FIG. 15. Estimated velocity errors, vorticity errors, and rates of convergence for the second test problem.

shows the estimated errors for the second test problem and the estimated rates of convergence.

To test the validity of these extrapolation-based estimates, we also applied the same procedure to the first test problem, where the errors are known. Tables I–IV show the resulting estimated errors and rates of convergence compared to the true errors and rates of convergence.

Examining Tables I and II, we note that at least with the eighth-order cutoff function, the estimated velocity errors and rates of convergence agree quite well with the true error. For the vorticity error, this is only true before the first rezoning takes place. The first rezoning occurs *before* time  $t = 5$  when  $\delta = 2.2\sqrt{h}$  and between  $t = 5$  and  $t = 10$  when  $\delta = 2.75\sqrt{h}$ . That is why the estimated vorticity

TABLE I

Estimated Rates of Convergence and Errors for  $h = 0.0625$  Using Extrapolation Compared to the Actual Errors for  $h = 0.0625$  and Rates of Convergence Based on the Actual Errors

	$t = 0$	$t = 5$	$t = 10$	$t = 15$	$t = 20$
Actual velocity error	$5.730 \times 10^{-6}$	$8.387 \times 10^{-6}$	$1.269 \times 10^{-5}$	$1.572 \times 10^{-5}$	$1.764 \times 10^{-5}$
Extrapolation estimated vel. error	$5.986 \times 10^{-6}$	$8.239 \times 10^{-6}$	$1.236 \times 10^{-5}$	$1.467 \times 10^{-5}$	$1.594 \times 10^{-5}$
Rate of convergence for velocity	3.6	3.7	3.7	3.8	3.8
Extrapolation estimated rate of conv.	3.5	3.7	3.8	3.9	4.0
Actual vorticity error	0	$2.168 \times 10^{-5}$	$2.980 \times 10^{-5}$	$3.737 \times 10^{-5}$	$4.160 \times 10^{-5}$
Extrapolation estimated vort. error	—	$1.586 \times 10^{-5}$	$4.186 \times 10^{-5}$	$9.821 \times 10^{-5}$	$1.082 \times 10^{-4}$
Rate of convergence for vorticity	—	3.1	3.5	3.4	3.4
Extrapolation estimated rate of conv.	—	4.8	3.8	2.6	2.9

Note. Eighth-order cutoff function,  $\delta = 2.2\sqrt{h}$ .

TABLE II

Estimated Rates of Convergence and Errors Using Extrapolation Compared to the Actual Errors and Rates of Convergence Based on the Actual Errors

	$t = 0$	$t = 5$	$t = 10$	$t = 15$	$t = 20$
Actual velocity error	$2.850 \times 10^{-5}$	$4.059 \times 10^{-5}$	$5.956 \times 10^{-5}$	$7.180 \times 10^{-5}$	$7.811 \times 10^{-5}$
Extrapolation estimated vel. error	$3.130 \times 10^{-5}$	$4.327 \times 10^{-5}$	$6.444 \times 10^{-5}$	$8.115 \times 10^{-5}$	$9.110 \times 10^{-5}$
Rate of convergence for velocity	3.4	3.5	3.5	3.6	3.6
Extrapolation estimated rate of conv.	3.3	3.4	3.4	3.3	3.3
Actual vorticity error	0	$5.796 \times 10^{-5}$	$1.284 \times 10^{-4}$	$1.325 \times 10^{-4}$	$1.634 \times 10^{-4}$
Extrapolation estimated vort. error	—	$6.030 \times 10^{-5}$	$1.213 \times 10^{-4}$	$1.094 \times 10^{-4}$	$2.969 \times 10^{-4}$
Rate of convergence for vorticity	—	3.1	2.7	2.9	2.8
Extrapolation estimated rate of conv.	—	3.1	4.1	4.1	2.9

Note. Eighth-order cutoff function,  $\delta = 2.75\sqrt{h}$ .

error agrees well with the true error at  $t = 5$  when  $\delta = 2.75\sqrt{h}$  but *not so well* when  $\delta = 2.2\sqrt{h}$ . This is not really surprising, since the vorticity error is only a piecewise smooth function of time when rezoning is used; see Figs. 2a, 5a, 8a, and 11a. Thus, the assumptions used in the extrapolation are not valid in this case. In Tables III and IV we see that, when the infinite order cutoff function is used, the estimated velocity error agrees well with the actual error for  $t \leq 10$  when  $\delta = 0.4\sqrt{h}$  but not so well when  $\delta = 0.5\sqrt{h}$ . The estimated vorticity error again agrees well with the true error at  $t = 5$  for the larger value of  $\delta$ , since no rezoning has taken place at that time, but at later times the discrepancy is larger in this case. It is also possible that the velocity and vorticity errors are not accurately described by (39). Indeed, by plotting the exact vorticity error as a function of  $r$  at  $t = 0$  for different values of  $h$  we find that the vorticity error at a given point *changes sign infinitely many times* as  $h$  tends to zero, when we use the infinite order cutoff function, while the error at a given point is of constant sign for the eighth-order cutoff function. Hence, the extrapolation assumption is justified in the eighth-order case, but not in the infinite order case.

We would need to incorporate an oscillation factor, which would be difficult in practice.

To investigate this phase change in the vorticity error for the infinite order case we use the Fourier transform to express the smoothing error as

$$\int_{1/\delta}^{\infty} J_0(rs) \hat{\omega}(s, t) ((2\pi)^{-2} - \hat{\phi}(\delta s)) s ds, \quad (40)$$

where  $\hat{\omega}(s, t)$  and  $\hat{\phi}(\delta s)$  are the Fourier transforms of the vorticity and the cutoff function, respectively. In Test Problem 1, we have  $\hat{\omega}(s, 0) = 2^7 \cdot 7! J_8(s) / (2\pi s^8)$ , while

$$(2\pi)^2 \hat{\phi}(s) = \begin{cases} 1 & \text{for } 0 \leq s \leq 1 \\ (44 + 2s^2 - s^4)/45 & \text{for } 1 \leq s \leq 2 \\ (256 - 32s^2 + s^4)/180 & \text{for } 2 \leq s \leq 4 \\ 0 & \text{for } s \geq 4 \end{cases} \quad (41)$$

for Hald's infinite order cutoff function. If we plug this into (40) and integrate by parts several times we get the

TABLE III

Estimated Rates of Convergence and Errors Using Extrapolation Compared to the Actual Errors and Rates of Convergence Based on the Actual Errors

	$t = 0$	$t = 5$	$t = 10$	$t = 15$	$t = 20$
Actual velocity error	$2.280 \times 10^{-6}$	$1.150 \times 10^{-6}$	$1.207 \times 10^{-6}$	$1.295 \times 10^{-6}$	$1.379 \times 10^{-6}$
Extrapolation estimated vel. error	$2.223 \times 10^{-6}$	$1.280 \times 10^{-6}$	$1.271 \times 10^{-6}$	$1.186 \times 10^{-6}$	$1.100 \times 10^{-6}$
Rate of convergence for velocity	4.7	6.0	6.4	6.5	6.5
Extrapolation estimated rate of conv.	4.9	6.0	6.7	7.3	7.7
Actual vorticity error	0	$1.505 \times 10^{-5}$	$1.629 \times 10^{-5}$	$1.460 \times 10^{-5}$	$1.264 \times 10^{-5}$
Extrapolation estimated vort. error	—	$2.329 \times 10^{-5}$	$2.636 \times 10^{-5}$	$2.169 \times 10^{-6}$	$1.951 \times 10^{-6}$
Rate of convergence for vorticity	—	4.0	4.3	4.7	4.9
Extrapolation estimated rate of conv.	—	3.3	9.8	10.3	10.5

Note. Infinite order cutoff function,  $\delta = 0.4\sqrt{h}$ .

TABLE IV

Estimated Rates of Convergence and Errors Using Extrapolation Compared to the Actual Errors and Rates of Convergence Based on the Actual Errors

	$t = 0$	$t = 5$	$t = 10$	$t = 15$	$t = 20$
Actual velocity error	$1.824 \times 10^{-5}$	$1.660 \times 10^{-5}$	$2.135 \times 10^{-5}$	$2.403 \times 10^{-5}$	$2.445 \times 10^{-5}$
Extrapolation estimated vel. error	$2.846 \times 10^{-5}$	$2.873 \times 10^{-5}$	$3.895 \times 10^{-5}$	$5.241 \times 10^{-5}$	$6.543 \times 10^{-5}$
Rate of convergence for velocity	4.2	4.9	5.0	5.1	5.2
Extrapolation estimated rate of conv.	3.7	4.1	4.2	3.9	3.7
Actual vorticity error	0	$5.732 \times 10^{-5}$	$1.049 \times 10^{-4}$	$1.048 \times 10^{-4}$	$1.222 \times 10^{-4}$
Extrapolation estimated vort. error	—	$6.373 \times 10^{-5}$	$5.205 \times 10^{-4}$	$6.887 \times 10^{-4}$	$2.732 \times 10^{-3}$
Rate of convergence for vorticity	—	3.4	3.2	3.6	3.5
Extrapolation estimated rate of conv.	—	3.5	2.6	2.0	1.0

Note. Infinite order cutoff function,  $\delta = 0.5\sqrt{h}$ .

vorticity smoothing error at  $t = 0$ ,

$$\begin{aligned} \omega(r, 0) - \tilde{\omega}(r, 0) = & -14\delta^9 \sum_{n=0}^5 (n^2 + 3n + 2)(-r)^n \\ & (4096J_{5-n}(1/\delta)J_n(r/\delta) \\ & - 160J_{5-n}(2/\delta)J_n(2r/\delta) \\ & + J_{5-n}(4/\delta)J_n(4r/\delta)) + R(r, \delta), \end{aligned} \quad (42)$$

where

$$\begin{aligned} R(r, \delta) = & 2^7 \cdot 7! \int_{1/\delta}^{\infty} J_0(t) \left( \frac{r^8 J_8(rt) p(\delta^2 t^2)}{t^7} \right. \\ & - \frac{16\delta^2 r^7 J_7(rt) p'(\delta^2 t^2)}{t^6} \\ & \left. + \frac{112\delta^4 r^6 J_6(rt) p''(\delta^2 t^2)}{t^5} \right) \end{aligned} \quad (43)$$

and  $p(t) = \hat{\phi}(\sqrt{t})$ . To estimate the remainder term, we note that by using the Taylor series for Bessel functions,  $R(r, \delta) = O(r^{12})$  for  $r/\delta$  “small.” Numerical evaluation of (43), shows that  $R(r, \delta)$  is in fact negligible for  $r < 0.5$ . Then (42) clearly shows that the error oscillates as  $h$  tends to 0. However, when  $r$  is close to one, the remainder term is not negligible. In this case, we estimate  $R(r, \delta)$  by replacing the Bessel functions in (43) by the leading term of their asymptotic expansions. We find that  $R(r, \delta)$  is dominated by the integral of the first term in (43), which is of order  $O(\delta^7)$  for  $r = 1$ , and  $O(\delta^8)$  when  $r < 1$ . This is due to the fact that  $J_0(t)$  and  $J_8(rt)$  have the same asymptotic phase when  $r = 1$ , but not when  $r < 1$ . Therefore  $J_0(t)J_8(rt)$  is almost nonnegative for  $r = 1$ , making the integral larger. When  $r = 0$ , the error (42) becomes  $-28\delta^9(4096J_5(1/\delta) - 160J_5(2/\delta) + J_5(4/\delta))$ .

For the eighth-order cutoff function, the vorticity smoothing error at  $t = 0$  is

$$\begin{aligned} \omega(r, 0) - \tilde{\omega}(r, 0) = & -\frac{\delta^8}{68} + \frac{\delta^{10}}{102} - \frac{5\delta^{12}}{1938} \\ & + \frac{\delta^{14}}{3876} + \left( \frac{15\delta^8}{68} - \frac{2\delta^{10}}{17} \right. \\ & \left. + \frac{35\delta^{12}}{1938} \right) r^2 + \left( \frac{-45\delta^8}{68} \right. \\ & \left. + \frac{7\delta^{10}}{34} \right) r^4 + \frac{35\delta^8 r^6}{68} \quad \text{for } r < \delta. \end{aligned} \quad (44)$$

When  $\delta$  is small enough, we can neglect powers of  $\delta$  higher than eight. Then the error is approximated by  $-\delta^8(1 - 15r^2 + 45r^4 - 35r^6)/68$  which has constant sign for fixed  $r$  as  $\delta$  tends to zero. Hence, the extrapolation assumption is valid in this case, at least for  $t = 0$ .

In the third test problem, the support of the initial vorticity is a square centered at the origin with the initial vorticity given by

$$\omega(x, y, 0) = (\max(0, 1 - x^2) \max(0, 1 - y^2))^7. \quad (45)$$

We again use the infinite order cutoff function, but now with  $\delta = 0.6\sqrt{h}$ . The viscosity is the same as in the previous problems. Figure 16 shows the positions of marker particles at different times and Fig. 17 shows the estimated rates of convergence.

We note that the estimated rates of convergence are somewhat lower than in the previous problems. This seems to be a consequence of using a slightly larger value of  $\delta$ , compared to the first test problem. If we use, instead,  $\delta = 0.4\sqrt{h}$  or  $\delta = 0.5\sqrt{h}$ , we get the same rates of convergence as in the first test problem at  $t = 0$ , but at later times the rates drop off significantly, even though rezoning is applied.

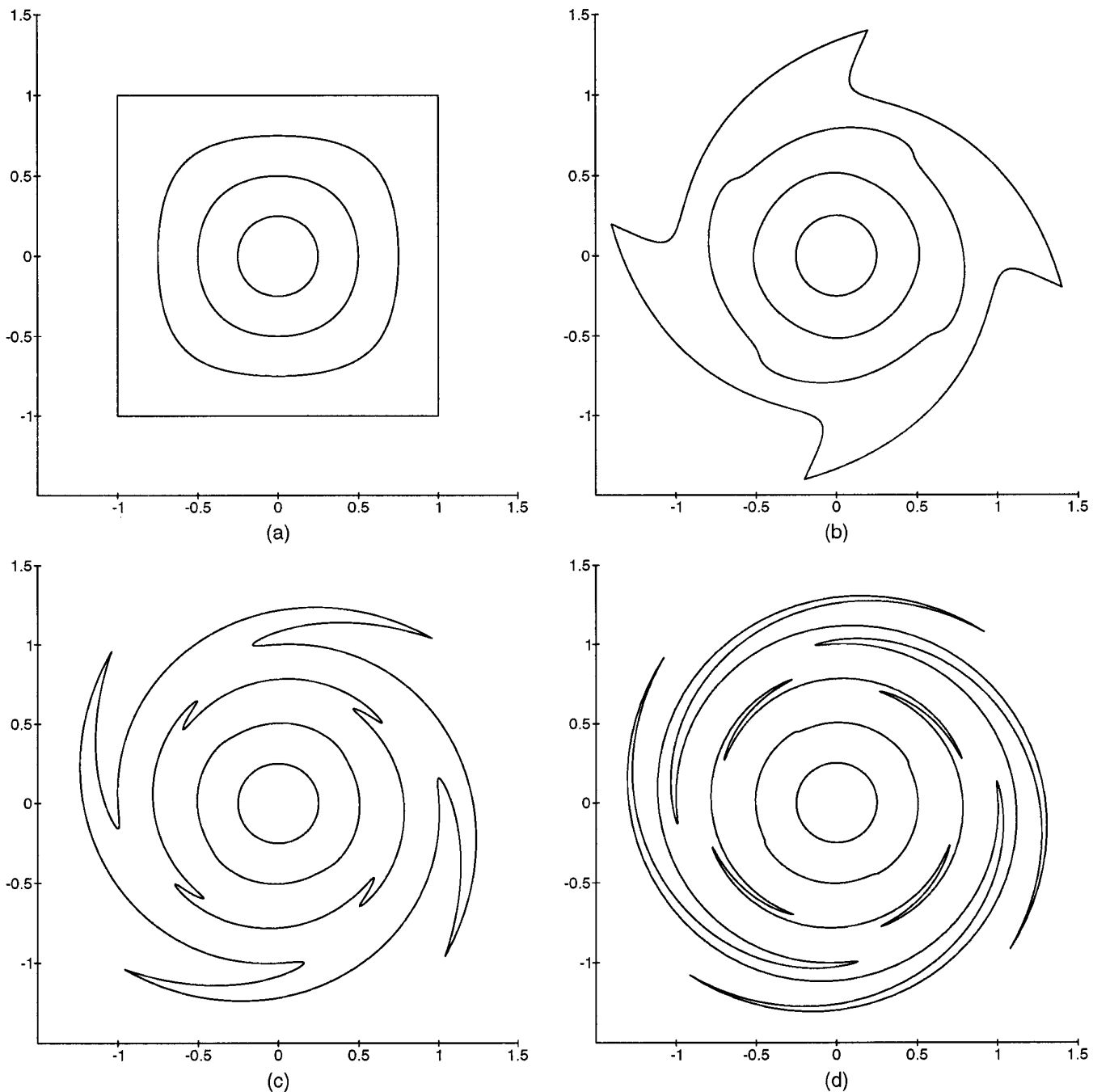


**FIG. 16.** Particle positions at  $t = 0$  (a),  $t = 20$  (b),  $t = 50$  (c),  $t = 100$  (d) with infinite order cutoff function.  $\omega(x, y, 0) = (\max(0, 1 - x^2) \max(0, 1 - y^2))^7$ ,  $h = 0.0625$ ,  $\delta = 0.6\sqrt{h}$ ,  $\Delta t = 4.0h$ .

I suspect that this is related to the fact that the support of the initial vorticity has a boundary with cusps.

#### 4. CONCLUSIONS

We have demonstrated that the application of automatic rezoning to deterministic high order vortex methods for

the Navier–Stokes equations gives numerical results which are at least as good as those obtained for the Euler equations in [11]. In the first test problem, we have, unlike other authors, measured the vorticity and velocity errors directly, rather than simply measuring the error in the functional  $L(t) = \int_{R^2} |\mathbf{x}|^2 \omega(\mathbf{x}, t) d\mathbf{x} / \int_{R^2} \omega(\mathbf{x}, t) d\mathbf{x}$ , which satisfies  $L(t) = L(0) + 4\nu t$ . This was possible thanks to the repre-

Rate of Convergence

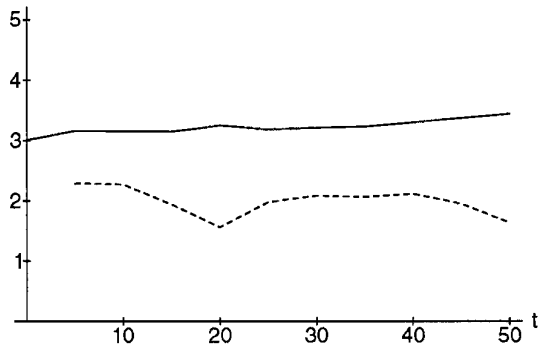


FIG. 17. Estimated rates of convergence for the third test problem.

sentation of the vorticity and angular velocity in terms of convergent series, derived by the author.

The reason why we have only chosen free-space problems, is that vortex methods cannot treat boundary conditions very accurately. So far, the best way to approximate boundary conditions has been to use vorticity creation at the boundary. Unfortunately, this process is inaccurate, and the errors introduced would totally dominate the other errors, making the use of a high order vortex method pointless.

## ACKNOWLEDGMENTS

The author gives special thanks to John Strain for many helpful and interesting suggestions. The author also thanks Ole Hald for interesting discussions.

## REFERENCES

1. J. T. Beale and A. Majda, *J. Comput. Phys.* **58**, 188 (1985).
2. A. J. Chorin, *J. Fluid Mech.* **57**, 785 (1973).
3. G. H. Cottet, *Math. Comput.* **56**, 45 (1991).
4. D. Fishelov, *J. Comput. Phys.* **86**, 211 (1990).
5. G. H. Cottet and S. MasGalic, *Numer. Math.* **57**, 805 (1990).
6. J. Goodman, *Commun. Pure Appl. Math.* **60**(2), 189 (1977).
7. O. H. Hald, *SIAM J. Numer. Anal.* **24**, 538 (1987).
8. T. Y. Hou, J. Lowengrub, and M. J. Shelley, *SIAM J. Sci. Comput.* **14**, 12 (1993).
9. D. G. Long, *J. Amer. Math. Soc.* **1**(4), 779 (1988).
10. F. Milinazzo and P. G. Saffman, *J. Comput. Phys.* **23**, 380 (1977).
11. H. O. Nordmark, *J. Comput. Phys.* **97**, 366 (1991).
12. H. O. Nordmark, CINVESTAV Matemáticas report, 1993 (unpublished).
13. M. Perlman, *J. Comput. Phys.* **59**, 200 (1985).
14. S. Roberts, *J. Comput. Phys.* **58**, 29 (1985).
15. L. Rosenhead, *Proc. R. Soc. London Ser. A* **134**, 170 (1932).